Molecular Vision 2017; 23:853-871 <http://www.molvis.org/molvis/v23/853>
Received 11 April 2017 | Accepted 3 December 2017 | Published 5 December 2017

Association of HMGB1 with oxidative stress markers and regulators in PDR

Ahmed M. Abu El-Asrar,[1,2] Kaiser Alam,[1] Marta Garcia-Ramirez,[3] Ajmal Ahmad,[1] Mohammad Mairaj Siddiquei,[1] Ghulam Mohammad,[1] Ahmed Mousa,[1] Gert De Hertogh,[4] Ghislain Opdenakker,[5] Rafael Simó[3]

(The first two and last two authors contributed equally to this study)

[1]Department of Ophthalmology, College of Medicine, King Saud University, Riyadh, Saudi Arabia; [2]Dr. Nasser Al-Rashid Research Chair in Ophthalmology, Riyadh, Saudi Arabia; [3]Diabetes and Metabolism Research Unit and CIBERDEM (ISCIII). Vall d'Hebron Research Institute. Barcelona, Spain; [4]Laboratory of Histochemistry and Cytochemistry, University of Leuven, KU Leuven, Leuven, Belgium; [5]Rega Institute for Medical Research, Department of Microbiology and Immunology, University of Leuven, KU Leuven, Leuven, Belgium

Purpose: We investigated the link among the proinflammatory cytokine high-mobility group box 1 (HMGB1) and 8-hydroxy-2'-deoxyguanosine (8-OHdG) as a marker of oxidative DNA damage, the endothelial adhesion molecule and oxidase enzyme vascular adhesion protein-1 (VAP-1), and the inducible cytoprotective molecule heme oxygenase-1 (HO-1) in proliferative diabetic retinopathy (PDR). We correlated the levels of these molecules with clinical disease activity and studied the proinflammatory activities of HMGB1 on rat retinas and human retinal microvascular endothelial cells (HRMECs).

Methods: Vitreous samples from 47 PDR and 19 non-diabetic patients, epiretinal membranes from 11 patients with PDR, human retinas (16 from diabetic patients and 16 from non-diabetic subjects), rat retinas, and HRMECs were studied by enzyme-linked immunosorbent assay, immunohistochemistry, western blot immunofluorescence, and RT-PCR analyses. In addition, we assessed the adherence of leukocytes to HMGB1-stimulated HRMECs.

Results: HMGB1, 8-OHdG, and soluble VAP-1 (sVAP-1) levels were significantly higher in vitreous samples from PDR patients than in those from non-diabetics ($p = 0.001$, <0.0001, <0.0001, respectively). The HMGB1, 8-OHdG, sVAP-1, and HO-1 levels in PDR with active neovascularization were significantly higher than those in inactive PDR ($p = 0.025$, <0.0001, <0.0001, 0.012, respectively). Significant positive correlations were observed between the levels of HMGB1 and the levels of 8-OHdG ($r = 0.422$; $p = 0.001$) and sVAP-1 ($r = 0.354$; $p = 0.004$) and between the levels of 8-OHdG and the levels of sVAP-1 ($r = 0.598$; $p<0.0001$). In epiretinal membranes, VAP-1 and 8-OHdG were expressed in vascular endothelial cells and stromal cells. Significant increases in the VAP-1 mRNA and protein levels were detected in the RPE, but not in the neuroretina of diabetic patients. Treatment of HRMEC with HMGB1, diabetes induction, and an intravitreal injection of HMGB1 in normal rats induced a significant upregulation of the adhesion molecule intercellular adhesion molecule-1 (ICAM-1) in HRMECs and retinas. On the other hand, the expressions of vascular cell adhesion molecule-1 and VAP-1 were not affected. Oral administration of the HMGB1 inhibitor glycyrrhizin in rats attenuated the diabetes-induced upregulation of the retinal ICAM-1 expression. Treatment of HRMECs with HMGB1 increased leukocyte adhesion and induced the upregulation of 8-OHdG and HO-1 and the membranous translocation of VAP-1.

Conclusions: Our results suggest a potential link among the proinflammatory cytokine HMGB1, VAP-1, oxidative stress, and HO-1 in the pathogenesis of PDR.

Diabetic retinopathy is characterized by progressive retinal endothelial cell dysfunction, the breakdown of the blood-retinal barrier, ischemia, and ischemia-induced retinal neovascularization. Retinal angiogenesis and the outgrowth of fibrovascular epiretinal membranes at the vitreo-retinal interface are the hallmarks of proliferative diabetic retinopathy (PDR) and are major contributors to vision loss due to vitreous hemorrhage or traction retinal detachment.

Increasing evidence suggests that oxidative stress and inflammation contribute to the pathogenesis of diabetes-induced retinal vasculopathy. Oxidative stress and associated reactive oxygen species (ROS) initiate inflammation in retinal endothelial cells, resulting in endothelial cell damage, increased microvascular permeability, and the increased recruitment of leukocytes [1,2]. Endothelial cell activation and the enhanced adhesion of leukocytes to the retinal endothelium are two of the earliest changes associated with diabetic retinopathy and they are involved in the

Correspondence to: Ahmed M. Abu El-Asrar, Department of Ophthalmology, King Abdulaziz University Hospital, Old Airport Road, P.O. Box 245, Riyadh 11411, Saudi Arabia, Phone: +966-11-4775723; FAX: +966-11-4775724; email: abuasrar@KSU.edu.sa / abuelasrar@yahoo.com

pathogenesis of retinal endothelial cell injury and the breakdown of the blood-retinal barrier. Retinal leukocyte stasis and the adhesion of leukocytes to the vascular wall correlate with the increased expression of retinal intercellular adhesion molecule-1 (ICAM-1) [3,4].

We demonstrated in several studies the overexpression of oxidative stress markers and proinflammatory and pro-angiogenic molecules in the ocular microenvironment of patients with PDR [5-12]. Pathologic angiogenesis is closely associated with the mobilization of inflammatory cells [13]. In several studies, it was shown that the fibrovascular epiretinal membranes surgically excised from patients with PDR are composed of new blood vessels, α-smooth muscle actin (α-SMA)-expressing myofibroblasts, and leukocytes expressing the common leukocyte antigen CD45 and the myeloid marker CD11b [5,6,10,11]. These findings suggest that oxidative stress, persistent inflammation, and neovascularization are critical for PDR initiation and progression. The causal relationships between inflammation and angiogenesis [14,15] and between oxidative stress and angiogenesis [13,16] are widely accepted.

The high-mobility group box 1 (HMGB1) protein is a highly abundant and conserved protein that has important biologic activities inside and outside the cell. Inside the nucleus, HMGB1 is known as a non-histone DNA binding protein that is involved in nucleosome stabilization and gene transcription. HMGB1 can be actively released from cells of the macrophage/monocyte lineage and mature dendritic cells following activation by proinflammatory stimuli. The protein is also passively released from necrotic ells, but not by cells undergoing apoptosis. Once released into extracellular milieu, HMGB1 functions as a proinflammatory cytokine that triggers inflammation and recruits leukocytes to the site of tissue damage [17-24], and it exhibits angiogenic effects [25-29]. Several receptors have been implicated in HMGB1-mediated signal transduction, cellular activation, and ensuing biologic functions. These include the receptor for advanced glycation end products (RAGE) and toll-like receptors. Signaling through these receptors leads to the activation of the extracellular signal-regulated kinase 1 and 2 (ERK1/2) signaling pathway and the transcription factor nuclear factor-kappa B (NF-κB). This leads to the upregulation of proinflammatory cytokines, chemokines, and adhesion molecules and intensifies cellular oxidative stress [12,18,19,21-24,30], processes that greatly contribute to the pathogenesis of diabetic retinopathy development and progression [1-4].

Increasing evidence in both clinical and experimental studies has indicated the central and causal role of HMGB1 in the pathogenesis of diabetic retinopathy. The expressions of HMGB1 and RAGE are upregulated in the ocular microenvironment of patients with PDR and in the retinas of diabetic animals [8,31-33]. In addition, HMGB1 mediates inflammation, oxidative stress, the breakdown of the blood-retinal barrier, and neuropathy in diabetic retinas [12,32-35]. This is partly mediated via RAGE [32,34]. These findings suggest that HMGB1 might provide a mechanistic link between chronic, low-grade subclinical inflammation and angiogenesis and between oxidative stress and angiogenesis in the ocular microenvironment of patients with PDR.

Novel markers and regulators of oxidative stress include 8-hydroxy-2'-deoxyguanosine (8-OHdG) [36-39], vascular adhesion protein-1 (VAP-1) [40-45], and heme oxygenase-1 (HO-1) [46-50]. After repair of ROS-mediated DNA damage, 8-OHdG is generated and is considered a biomarker of oxidative damage to DNA, because among the four nucleobases, guanosine is the most susceptible to oxidation. Oxidative DNA damage is considered detrimental, as the replication of damaged DNA can lead to genetic mutations or apoptosis [36-38]. In a meta-analysis, the levels of 8-OHdG were found to be associated with cardiovascular disease [36]. In diabetic nephropathy, 8-OHdG was found to be an excellent marker of oxidative stress. This molecule originates from intracellular sources and becomes an extracellular analyte in the urine [39]. VAP-1 is expressed as a transmembrane glycoprotein in the vascular wall and it supports the rolling, firm adhesion, and transmigration of various subsets of leukocytes to sites of inflammation. It is recognized by the lectin Siglec 10 on leukocytes. VAP-1 is one of the members of the copper-containing amine oxidase/semicarbazide-sensitive amine oxidase (AOC/SSAO) enzyme family. These enzymes catalyze the oxidative deamination of primary amines, which results in the production of the corresponding aldehyde, hydrogen peroxide, and ammonia. These products activate NF-κB-dependent chemokine secretion and adhesion molecule expressions, and they initiate and propagate oxidative stress. VAP-1, therefore, operates as an adhesion molecule and as an oxidase enzyme. VAP-1 is present in either a membrane or a soluble (sVAP-1) form [40-42]. The VAP-1/SSAO reaction results in the generation of bioactive compounds. Among the end products, hydrogen peroxide is a major ROS and the main generator of oxidative stress [42]. VAP-1 can modulate leukocyte migration in both its transmembrane and soluble forms. It was demonstrated that hydrogen peroxide is the main mediator of VAP-1 enzyme catalytic activity in the expression of endothelial selectins, the binding of leukocytes to endothelial cells, leukocyte migration, and the inflammatory function of VAP-1 [41,43-45]. HO-1 is the inducible enzyme catalyzing the oxidation of heme to generate carbon monoxide, biliverdin, and ferrous

iron. These reaction products of HO-1 have potent anti-inflammatory and anti-oxidative functions. HO-1 is highly inducible in response to numerous stimuli causing oxidative stress to protect cells against apoptotic, oxidative, and inflammatory injury [46,47]. HO-1 is essentially an intracellular protein that is induced in diabetic rat retinas [48]. As such, it has never been analyzed in vitreous fluids, but it was found to be present in the retinal lysates of diabetic rats [48,49]. In the biomarker field, extracellular HO-1 levels have been detected, for instance, in the urine of diabetics as an early marker of diabetic injury [50]. For these reasons, it was interesting to evaluate HO-1 levels in vitreous samples.

The aim of this study was to investigate the potential link between the proinflammatory cytokine HMGB1 and the biomarker of oxidative DNA damage 8-OHdG, the endothelial adhesion molecule and oxidase enzyme VAP-1, and the inducible cytoprotective molecule HO-1 in PDR. In addition, we studied the proinflammatory activities of HMGB1 on rat retinas and human retinal microvascular endothelial cells (HRMECs).

METHODS

Vitreous samples and epiretinal membrane specimens: We studied undiluted vitreous fluid samples obtained from 47 patients with PDR during pars plana vitrectomy. The indications for vitrectomy were tractional retinal detachment or non-clearing vitreous hemorrhage. The severity of retinal neovascular activity was graded clinically at the time of vitrectomy using previously published criteria [51]. PDR was considered active if there were visible perfused new vessels on the retina or optic disc and within the tractional epiretinal membranes. PDR was considered inactive (involuted) if only non-vascularized, white fibrotic epiretinal membranes were present. Active PDR was present in 25 patients, and inactive PDR was present in 22 patients. The diabetic patients were 32 males and 15 females whose ages ranged from 27 to 72 years, with a mean of 52.1 ± 11.4 years. The duration of diabetes ranged from six to 30 years, with a mean of 16.2 ± 5.4 years. The total PDR group consisted of a subgroup of 17 patients who had insulin-dependent diabetes mellitus and another group of 30 patients who had non-insulin-dependent diabetes mellitus. The control group consisted of 19 patients who had undergone vitrectomy for the treatment of rhegmatogenous retinal detachment with no proliferative vitreoretinopathy. Controls were free from systemic disease. Epiretinal fibrovascular membranes were obtained from 11 patients with PDR during pars plana vitrectomy for the repair of tractional retinal detachment. Membranes were fixed for 2 h in 10% formalin solution and embedded in paraffin.

The study was conducted according to the tenets of the Declaration of Helsinki. All patients were candidates for vitrectomy as a surgical procedure, and all patients signed preoperative informed written consent and approved of the use of the excised epiretinal membranes and vitreous fluid for further analysis and clinical research. The study design and the protocol were approved by the Research Centre and Institutional Review Board of the College of Medicine, King Saud University.

Human postmortem eyes: Human postmortem eyes were obtained from 16 diabetic and 16 non-diabetic (control group) donors matched by age (67 ± 8 years and 68 ± 6 years, respectively). The time elapsed from death to eye enucleation was 3.4 ± 1.9 h. After enucleation, one eye of each donor was snap-frozen in liquid nitrogen and stored at -80 °C until they were assayed for mRNA and western blot analyses. The other eye was fixed in 4% paraformaldehyde and embedded in paraffin for the immunofluorescence study.

After thawing, the neuroretina and RPE were quickly harvested. The vitreous and neuroretina were removed and the RPE layer was then carefully peeled off from Bruch's membrane using forceps (Dumont No 5, Sigma, Madrid, Spain) under the dissecting microscope (Olympus SZ61, Barcelona, Spain).

All ocular tissues were obtained and used in accordance with applicable laws of the Diabetes and Metabolism Research Unit and CIBERDEM (ISCIII), Vall d'Hebron Research Institute, Barcelona, Spain, and following the Declaration of Helsinki for research involving human tissue. In addition, this study was approved by the Hospital Ethics Committee of Vall d'Hebron, Barcelona, Spain.

Induction of diabetes and glycyrrhizin treatment: All procedures with animals were performed in accordance with the Association for Research in Vision and Ophthalmology (ARVO) statement for use of animals in ophthalmic and vision research and they were approved by the institutional animal care and use committee of the College of Pharmacy, King Saud University. Adult male Sprague Dawley rats 7–10 weeks of age (200−220 g) were overnight fasted and a single bolus dose of streptozotocin (STZ) 55 mg/kg in 10 mM sodium citrate buffer, pH 4.5 (Sigma, St. Louis, MO), was injected intraperitoneally. Equal volumes of citrate buffer were injected in age-matched control rats. Rats were considered diabetic if their blood glucose was greater than 250 mg/dl.

Diabetic rats were divided into two groups: the rats in group I received normal drinking water without any supplementation and those in group II (curative treatment scheme, after disease induction) received drinking water

supplemented with the potent HMGB1 inhibitor glycyrrhizic acid [52] (150 mg/kg/day, Santa Cruz Biotechnology Inc., Santa Cruz, CA) immediately after the establishment of diabetes [32-35]. After fou r weeks of diabetes, the rats were euthanized by an overdose of chloral hydrate, the eyes were removed, and the retinas were isolated and frozen immediately in liquid nitrogen and stored at -80 °C until analyzed.

Intravitreal injection of HMGB1: Sprague Dawley rats (220–250 g) were kept under deep anesthesia, and a sterilized solution of recombinant HMGB1 (5 ng/5 µl; R&D Systems, Minneapolis, MN) was injected into the vitreous of the right eye as previously described [32-35]. For the control, the left eye received 5 µl of sterile PBS (10 mM sodium phosphate ,150 mM sodium chloride, pH 7.8±0.2). Each group had 7–10 rats. The animals were sacrificed four days after intravitreal administration, and the retinas were carefully dissected, snap frozen in liquid nitrogen, and stored at -80 °C until analyzed.

Cell culture: HRMECs were purchased from Cell Systems Corporation (Kirkland, WA) and maintained in complete serum-free media (Cat. No. SF-4Z0–500, Cell System Corporation) supplemented with "Rocket Fuel" (Cat No. SF-4Z0–500, Cell System Corporation), "Culture Boost" (Cat. No. 4CB-500, Cell System Corporation), and antibiotics (Cat. No. 4Z0–643, Cell System Corporation) at 37 °C in a humidified atmosphere with 5% CO_2. We used HRMECs up to passage 8 for all the experiments. About 80% confluent cells were starved in a minimal medium (medium supplemented with 0.25% "Rocket Fuel" and antibiotics) overnight to eliminate any residual effects of growth factors. Following starvation, HRMECs were either left untreated or treated with 100 ng/ml of cytokine-HMGB1, lipopolysaccharide free (Cat. No. REHM120, IBL International Corporation, Toronto, ON). Cells were harvested after 24 h and lysed in radioimmunoprecipitation assay (RIPA) lysis buffer (sc-24948, Santa Cruz Biotechnology, Dallas, TX) for western blot analysis.

Enzyme-linked immunosorbent assays for vitreous samples: Enzyme-linked immunosorbent assay (ELISA) kits for human sVAP-1 (Cat No: ab-119564) and human 8-OHdG (Cat No: ab-101245) were purchased from Abcam, Cambridge, UK. The ELISA kit for human HO-1 (Cat No: KCB3776) was purchased from R&D Systems and the ELISA kit for human HMGB1 (Cat No: ST5101) was purchased from IBL International GMBH, Hamburg, Germany. The ELISA plate readings were done using a Stat Fax-4200 microplate reader from Awareness Technology, Inc., Palm City, FL. The levels of human sVAP-1, 8-OHdG, HO-1, and HMGB1 in vitreous fluid samples were determined based on the standards and protocols provided by the manufacturers.

Western blot analysis of human vitreous fluid and rat retinas: Retinas and cells were homogenized in a western lysis buffer (30 mM Tris-HCl; pH 7.5, 5 mM EDTA, 1% Triton X-100, 250 mM sucrose, 1 mM sodium vanadate and protease inhibitor cocktail), the lysates were then centrifuged at 14,000 ×*g* for 15 min at 4 °C, and the supernatant was used for protein estimation and further analysis. Equal amounts of protein were subjected to sodium dodecyl sulfate–polyacrylamide gel electrophoresis (SDS-PAGE) in 8%–10% gels and transferred onto nitrocellulose membranes (Bio-Rad Laboratories). To determine the presence of VAP-1 in the vitreous samples, equal volumes (15 µl) of vitreous samples were boiled in Laemmli's sample buffer (1:1, v/v) under reducing conditions for 10 min and analyzed as described (6,10,11). Immunodetection was performed with the use of the anti-VAP-1 antibody (1:1000, ab196739, Abcam), anti-ICAM-1 antibody (1:500; sc 8439, Santa Cruz, Biotechnology Inc.), and anti-vascular cell adhesion molecule-1 (VCAM-1) antibody (1:500, sc 13,160, Santa Cruz, Biotechnology Inc.). Membranes were stripped and re-probed with an antibody against β-actin to evaluate sample processing and lane loading. Bands were visualized using a high-performance chemiluminescence machine (G: Box Chemi-XX8 from Syngene, Synoptic Ltd. Cambridge, UK), and the intensities were quantified using the GeneTools software (Syngene by Synoptic Ltd.).

Immunohistochemical staining of epiretinal membranes: For CD31 and α-SMA, antigen retrieval was performed by boiling the sections in citrate-based buffer (pH 5.9–6.1; BOND Epitope Retrieval Solution 1; Leica) for 10 min. For CD45, VAP-1, and 8-OHdG detection, antigen retrieval was performed by boiling the sections in Tris/EDTA buffer (pH 9; BOND Epitope Retrieval Solution 2; Leica) for 20 min. Subsequently, the sections were incubated for 60 min with mouse monoclonal anti-CD31 (ready-to-use; clone JC70A; Dako, Glostrup, Denmark), mouse monoclonal anti-CD45 (ready-to-use; clones 2B11+PD7/26; Dako), mouse monoclonal anti-α-SMA (ready-to-use; clone 1A4; Dako), rabbit polyclonal anti-VAP-1 antibody (1:100; ab135695, Abcam), and mouse monoclonal anti-8-OHdG (1:50; ab26842, Abcam). Optimal working concentrations and incubation times for the antibodies were determined earlier in pilot experiments. The sections were then incubated for 20 min with a secondary IgG conjugated with alkaline phosphatase. The reaction product of the enzyme was visualized by incubation for 15 min with the Fast Red chromogen, resulting in bright-red immunoreactive sites. The slides were then faintly counterstained with Mayer's hematoxylin (BOND) Polymer Refine Red Detection Kit (Leica). Negative controls were identified by omission of the primary antibody from the staining protocol. Instead, the ready-to-use DAKO Real Antibody Diluent (Agilent

Technologies product code S2022) was applied. To identify the phenotype of stromal cells expressing VAP-1, sequential double immunohistochemistry was performed as described [5,6,10,11].

Immunofluorescence for VAP-1 in the retinas of human subjects with diabetes mellitus: Paraffinized eyes were cut at a thickness of 7 µm. Sections were deparaffinized with xylene, rehydrated in ethanol, washed in PBS, and placed in an antigen-retrieval solution (Dako A/S, Glostrup, Denmark). Permanganate bleaching was used to eliminate the autofluorescence of the RPE. Sections were then incubated for 1 h with 2% BSA in 0.05% Tween in PBS to block unspecific binding and then incubated overnight at 4 °C with the anti-VAP-1 antibody (1:500; ab115574, Abcam, Madrid, Spain) or anti-collagen IV (1:200; ab6586, Abcam, Madrid, Spain). After washing, sections were incubated with Alexa Fluor 488 and 594 secondary antibodies (Molecular Probes, Invitrogen, Madrid, Spain) at room temperature for 1 h. Slides were coverslipped with a mounting medium containing 4′, 6-diamidino-2-phenylindole (DAPI) for the visualization of cell nuclei (Vector Laboratories, Palex, Sant Cugat del Vallés, Spain). Images were acquired with a confocal scanning microscope (FV1000, Olympus, Hamburg, Germany).

Protein extraction and western blot analysis of the VAP-1 expression in the retinas of human subjects with diabetes mellitus: RPE and neuroretina samples were extracted with a RIPA buffer (1% Triton X-100, 100 mmol/l Tris-HCl, pH 7.5; 150 mmol/l NaCl; 1.5 mmol/l EDTA, pH 8.0; 25 mmol/l NaF; 0.5 mmol/l Na_3VO_4; 0.1 mmol/l phenylmethylsulfonyl fluoride; and Complete protease inhibitors [Roche, Basel, Switzerland]) and homogenized by sonication. Protein concentrations were determined using bicinchoninic acid assay (Bio-Rad Laboratories, Madrid, Spain). Equivalent amounts (20 µg) of total protein extracts were resolved by 10% SDS-PAGE and transferred to ECL nitrocellulose membranes (Hybond, Amersham Pharmacia Biotech). The membranes were incubated with a primary antibody against VAP-1 (1:1000; ab115574, Abcam, Madrid, Spain) and further incubated with a peroxidase-conjugated secondary antibody (Bio-Rad Laboratories, Madrid, Spain). Membranes were stripped and re-probed with β-actin to evaluate the lane-loading control. Proteins were visualized using the enhanced chemiluminescence detection system ECL (Advansta, CA).

RNA extraction and quantitative real-time PCR of the VAP-1 expression in the retinas from human subjects with diabetes mellitus: The human neuroretina (NR) and RPE of isolated eyecups from human donors were harvested by dissection under the microscope. Total RNA was extracted from isolated retinal tissues using the Trizol reagent (Invitrogen, Barcelona, Spain) according to the manufacturer's instructions. RNA quantity was measured on a NanoDrop spectrophotometer and integrity was determined on an Agilent 2100 Bioanalyzer. Reverse transcription was performed with a High Capacity Kit (Applied Biosystems, Madrid, Spain) with random hexamer primers. RT-PCR was performed with the use of the SYBR Green PCR Master Mix (Applied Biosystems, Warrington, UK) in the 7.900 HT Sequence Detection System with 384-well optical plates. The specific primers were for hVAP-1: 5′-CAA TGA GAC CAT TGC TGG AA-3′ and 5′-TGT CCT CTG CAT GTG GGA TA-3′. For each sample, qPCR was performed in triplicate and relative quantities were calculated, and the ABI SDS 2.0 RQ software and the $2^{-\Delta\Delta Ct}$ analysis method with human β-actin (as the endogenous control; β-actin forward primer, 5′-TGG AGA AAA TCT GGC ACC AC-3′ and reverse primer, 5′-GAG GCG TAC AGG GAT AGC AC-3′) were used.

Cell adhesion assay: The adherence of human leukocytes to stimulated HRMEC monolayers was assessed. We used the CytoSelect Leukocyte-Endothelium Adhesion Assay kit (Cat. No. CBA-210, CELL BIOLABS, INC.) and followed the provided protocol exactly. Briefly, 1×10^5 HMRECs were seeded into each well of attachment factor-coated 96-well plates in 200 µl of a completely serum-free medium and grown for 48 h. Confluent monolayers of endothelial cells were starved overnight in a minimal medium. Starved HRMECs were left untreated or treated with different doses (2 ng/ml to 200 ng/ml) of cytokine-HMGB1, lipopolysaccharide free (Cat. No. REHM120, IBL International Corporation) or with 1 ng/ml recombinant human tumor necrosis factor-α (TNF-α, positive control; Cat. No. 210-TA, R&D Systems) for 24 h.

In the meantime, leukocytes were isolated from healthy volunteers by Ficoll-HISTOPAQUE-1077 (Cat. No. 10,771, Sigma-Aldrich) density gradient centrifugation. Briefly, in 15 ml conical tubes, 5.4 ml of the Ficoll HISTOPAQUE-1077 reagent was added and on top of this, 7.5 ml of 1:1 blood-PBS was slowly layered. Thereafter, the contents were centrifuged at 595 ×g for 30 min at room temperature and the buffy coats were carefully pipetted off into other conical tubes. Cells were pelleted by centrifugation at 393 ×g for 10 min and they were resuspended in Dulbecco's Modified Eagle Medium (DMEM) with 10% fetal bovine serum (FBS) and antibiotics. Peripheral blood leukocytes were labeled with the fluorescent LeukoTracker for 60 min at 37 °C, then counted by trypan blue exclusion assay, and immediately used for adhesion assay.

In total, 3×10^5 labeled leukocytes were added to each well of the control or treated HRMEC monolayers for 30 min

at 37 °C. After treatment with the washing buffer provided in the kit, the remaining adherent leukocytes were lysed in the lysis buffer of the kit. Fluorescence was measured using a spectraMax Gemini XPS (Molecular Devices, CA) with excitation and emission wavelengths of 485 nm and 538 nm, respectively.

Immunofluorescence staining and microscopy of HRMECs: HRMECs were cultured in coverslips in six-well plates and starved in minimal media overnight. They were left untreated or were treated with 100 ng/ml of cytokine-HMGB1, lipopolysaccharide free (Cat. No. REHM120, IBL International Corporation) for 24 h and were fixed with ice-cold acetone or 4% paraformaldehyde followed by blocking with 10% goat serum for 1 h. Without being washed, the cells were incubated with anti-HO-1 (1:100, sc-10789, Santa Cruz Biotechnology, Inc.), anti-VAP-1 (1:100, ab196739, Abcam), or anti-8OHdG (1:50, ab62623, Abcam) primary antibodies overnight at 4 °C. After washing, cells were incubated with secondary antibodies conjugated with appropriate fluorophores (Alexa Fluor 488 or 555) diluted in 10% goat serum (1:1000) for 1 h at room temperature. After washing, the cell-containing coverslips were counterstained with DAPI before being mounted on a glass slide with the use of the UltraCruz™ Mounting Medium (sc-24941, Santa Cruz Biotechnology Inc.). Immunofluorescence microscopy was performed using an Olympus motorized system microscope (BX61, Olympus Corporation, Tokyo, Japan) at 20X or 40X magnification.

Statistical analysis: Data are presented as the mean ± standard deviation (SD). The non-parametric Kruskal–Wallis test was used to compare means among active PDR patients, inactive PDR patients, and non-diabetic control patients. The non-parametric Mann–Whitney *U* test was used to compare means from two independent groups. Spearman's correlation coefficients were computed to investigate correlations between variables. A p value less than 0.05 was considered statistically significant, and SPSS version 20.0 for Windows (IBM Inc., Chicago, IL) was used for statistical analysis.

RESULTS

ELISA levels of HMGB1, 8-OHdG, sVAP-1, and HO-1 in vitreous samples and their relation with PDR activity and correlations: HMGB1, 8-OHdG, sVAP-1, and HO-1 were detected in all vitreous samples from patients with PDR and non-diabetic control patients. The mean HMGB1 level in PDR patients (7.59 ± 3.68 ng/ml) was significantly higher than the mean level in non-diabetic control patients (3.89 ± 3.22 ng/ml; p = 0.001). The mean 8-OHdG level in PDR patients (7.81 ± 4.86 ng/ml) was significantly higher than the mean level in controls (3.34 ± 1.43 ng/ml; p<0.0001). The mean sVAP-1 level in PDR patients (1,217 ± 590 pg/ml) was significantly higher than the mean level in controls (421 ± 144 pg/ml; p<0.0001). The mean HO-1 level in vitreous samples from PDR patients (236 ± 205 RFUs) was higher than that in control patients (178 ± 69 RFUs). However, the latter difference was not statistically significant (p = 0.805; Table 1).

Comparisons of the mean levels of HMGB1, 8-OHdG, sVAP-1, and HO-1 among active PDR patients, inactive PDR patients, and non-diabetic control patients were conducted with the Kruskal–Wallis test and the results are shown in Table 1. The mean levels differed significantly among the three groups for HMGB1 (p<0.0001), 8-OHdG (p<0.0001), sVAP-1 (p<0.0001), and HO-1 (p = 0.035). Pairwise comparisons (Mann–Whitney *U* test) indicated that the mean HMGB1 level was significantly higher in patients with active PDR than in inactive PDR and control patients (p = 0.025; p<0.0001, respectively). In addition, the mean HMGB1 level in patients

Table 1. Comparisons of mean HMGB1, 8-OHdG, sVAP-1 and HO-1 levels in proliferative diabetic retinopathy (PDR) patients with or without active neovascularization and nondiabetic patients with rhegmatogenous retinal detachment (RD).

Disease group	HMGB1 (ng/ml)	8-OHdG (ng/ml)	sVAP-1 (pg/ml)	HO-1 (RFUs)
All PDR (n=47)	7.59±3.68	7.81±4.86	1217.89±590.31	236.74±205.26
RD (n=19)	3.89±3.22	3.34±1.43	421.06±144.82	177.61±69.46
P value (Mann–Whitney test)	0.001*	<0.001*	<0.0001*	0.805
Active PDR (n=25)	8.86±4.24	11.02±4.53	1705.76±191.94	335.14±270.64
Inactive PDR (n=22)	6.08±2.13	4.16±1.46	663.50±340.37	165.18±95.75
RD (n=19)	3.89±3.22	3.34±1.43	421.06±144.82	177.61±69.46
P value (Kruskal–Wallis test)	<0.0001*	<0.0001*	<0.0001*	0.035*

*Statistically significant at 5% level of significance. HMGB1=high mobility group box-1; 8-OHdG=8-hydroxy-2'-deoxyguanosine; sVAP-1=soluble vascular adhesion protein-1; HO-1=heme oxygenase-1; RFUs=relative fluorescence units.

with inactive PDR was significantly higher than the mean level in control patients (p = 0.019). For 8-OHdG, the mean level was significantly higher in patients with active PDR than in inactive PDR and control patients (p<0.0001 for both comparisons). For sVAP-1, the mean level was significantly higher in patients with active PDR than in inactive PDR and non-diabetic patients (p<0.0001 for both comparisons). In addition, the mean sVAP-1 level in patients with inactive PDR was significantly higher than the mean level in control patients (p = 0.002). For HO-1, the mean level in patients with active PDR was significantly higher than in inactive PDR patients (p = 0.012).

Significant positive correlations (Spearman's correlation test) were found between the vitreous fluid levels of HMBG1 and the levels of 8-OHdG (r = 422; p = 0.001) and sVAP-1 (r = 0.354, p = 0.004). A significant positive correlation was observed between the vitreous fluid levels of sVAP-1 and 8-OHdG (r = 0.598; p<0.0001; Figure 1). In contrast, the correlations between the levels of HO-1 and levels of HMGB1, 8-OHdG, and sVAP-1 were not significant.

To obtain information about the molecular form of sVAP-1 and to compare its concentrations, we analyzed equal volumes (15 µl) of vitreous samples with the use of western blot analysis, and we confirmed that sVAP-1 was present in vitreous samples. Although the signal was rather weak, the protein in the samples migrated at the expected molecular weight, and the relative levels in PDR patients versus non-diabetic controls were in line with the ELISA data (Figure 2).

Immunohistochemical analysis of fibrovascular epiretinal membranes from patients with PDR: To identify the cell source of vitreous fluid sVAP-1 and 8-OHdG, fibrovascular epiretinal membranes from patients with PDR were studied by immunohistochemical analysis. No staining was observed in the negative control slides (Figure 3A). All membranes showed blood vessels that were positive for CD31 (Figure 3B), stromal cells expressing CD45 (Figure 3C), and stromal spindle-shaped cells expressing the myofibroblast marker α-SMA (Figure 3D). VAP-1 immunoreactivity was present in all membranes and was noted in vascular endothelial cells and stromal cells (Figure 4A-C). In addition, VAP-1 immunoreactivity was detected in stromal cells expressing CD45 and in spindle-shaped cells. In serial sections, the distribution and morphology of spindle-shaped cells expressing VAP-1 (Figure 4C) were similar to those of cells expressing α-SMA (Figure 3D). A double immunohistochemistry analysis confirmed that stromal cells expressing VAP-1 co-expressed CD45 (Figure 4D, E). Strong 8-OHdG immunoreactivity was detected in all cell types of the PDR fibrovascular epiretinal membranes, including endothelial and stromal cells. As well, 8-OHdG immunoreactivity was observed in the nuclear and cytoplasmic compartments of the cells (Figure 4F).

Effect of diabetes on the VAP-1 expression in retinas of human subjects with diabetes mellitus: The VAP-1 mRNA expression was higher in diabetic donors than in non-diabetic donors in the RPE (p = 0.03). On the other hand, the expression of VAP-1 mRNA did not differ significantly between non-diabetic donors and diabetic donors in the neuroretina (p = 0.81; Figure 5A). These findings were also confirmed at the protein level by western blot analysis (p = 0.04 for the RPE; p = 0.07 for the neuroretina; Figure 5B). VAP-1 immunofluorescence showed a higher expression of VAP-1 in the RPE of diabetic donors compared to non-diabetic donors (Figure 6A). A double immunofluorescence analysis revealed that VAP-1 immunostaining was co-localized with the basal lamina marker collagen IV in retinal vessels (Figure 6B).

Effect of diabetes and intravitreal administration of HMGB1 on the retinal expression of adhesion molecules: We tried to corroborate the findings in a preclinical rat model of streptozotocin-induced diabetes. The body weights of the diabetic rats were lower and their blood glucose levels were more than fourfold higher compared to the age-matched normal control rats (171 ± 20 versus 269 ± 27 g and 487 ± 31 versus 107 ± 10 mg/dl, respectively). Treatment of the diabetic rats with glycyrrhizin for one month did not change these metabolic variables in the diabetic rats (189 ± 29 versus 171 ± 20 g and 492 ± 28 versus 487 ± 31 mg/dl, respectively).

Western blot analysis of homogenized retinal tissue demonstrated that diabetes and an intravitreal injection of HMGB1 induced the significant upregulation of ICAM-1. Diabetes and an HMGB1 injection resulted in about 45% and 51% increases, respectively, in the ICAM-1 expression (Figure 7). On the other hand, the expressions of VCAM-1 and VAP-1 were not affected by diabetes or an intravitreal injection of HMGB1. Constant glycyrrhizin intake from the onset of diabetes significantly attenuated the diabetes-induced upregulation of ICAM-1 by about 44% (Figure 7), confirming that this compound acted in vivo.

HMGB1 induces leukocyte adhesion to HRMECs and the expression of cell adhesion molecules, 8-OHdG, and HO-1 in HRMECs: In the optimizing experiment, HRMECs were treated with different doses of HMGB1 (2 ng/ml to 200 ng/ml) for 24 h to activate the endothelial cells. Thereafter, LeukoTracker-labeled leukocytes were added and allowed to interact with the endothelial cells. The cultures were then gently washed and the remaining adhered leukocytes were quantified by measuring the amount of fluorescent labels in total cell lysates. We found that treatment of HRMECs with 100 ng/ml HMGB1 resulted in maximum adhesion of the

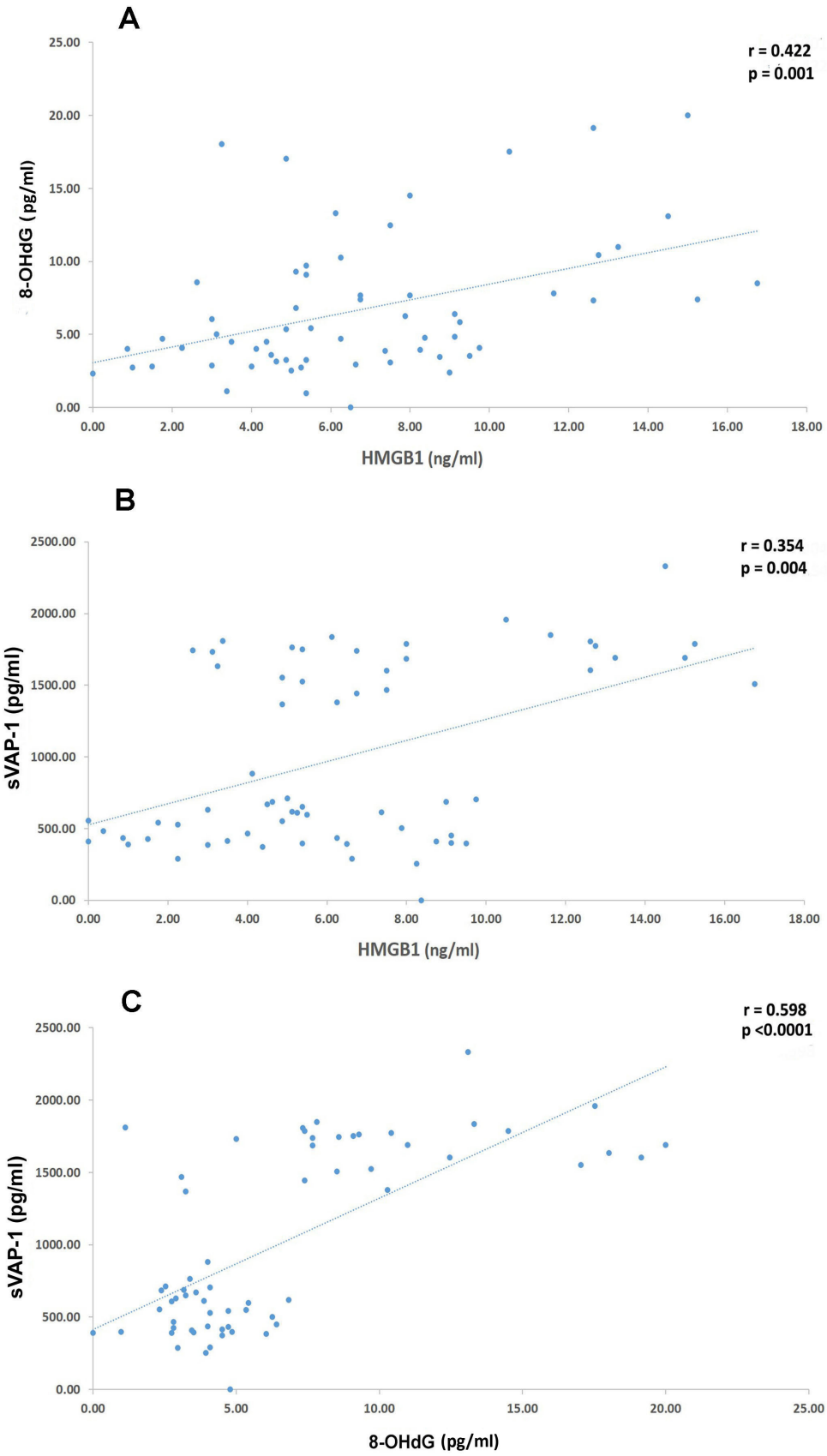

Figure 1. Spearman's correlation test. Significant positive correlations between the vitreous fluid levels of HMGB1 and levels of 8-OHdG **A**: and sVAP-1 and between **B:** vitreous fluid levels of 8-OHdG and **C:** levels of sVAP-1.

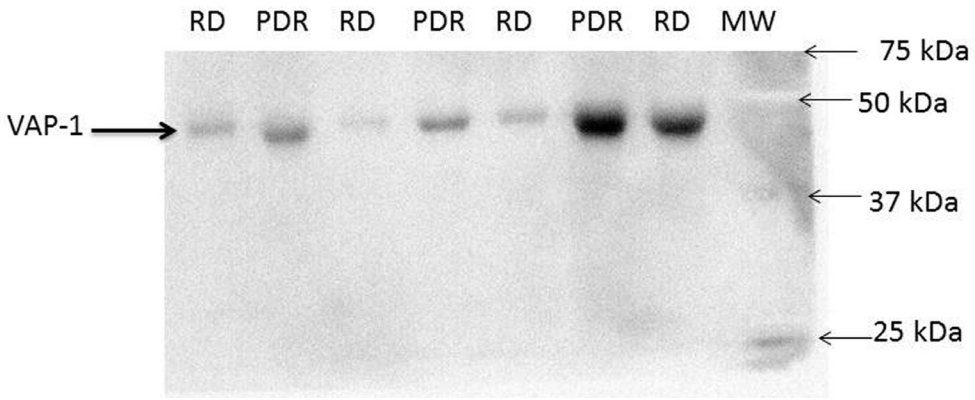

Figure 2. Western blot analysis of vitreous samples. The expression of sVAP-1 in equal volumes (15 µl) of vitreous fluid samples from patients with PDR and control patients without diabetes (RD) was determined by western blot analysis. A representative set of samples is shown.

leukocytes (Figure 8A). Therefore, we used this dose for all other in vitro experiments. We also used TNF-α (1 ng/ml) as a positive control. Our data revealed that 100 ng/ml HMGB1 significantly upregulated the adherence of human leukocytes to HRMECs (Figure 8B).

With the use of western blot analysis, we demonstrated that the treatment of HRMECs with HMGB1 (100 ng/ml) for 24 h resulted in an increased expression of ICAM-1 compared with the control medium. On the other hand, the expressions of VCAM-1 and VAP-1 were not affected by HMGB1 treatment (Figure 8C).

Immunofluorescence microscopy showed both cytoplasmic and membranous VAP-1 immunoreactivity in the untreated cells. The HMGB1-treated cells showed predominant membranous immunoreactivity (Figure 9A).

HO-1 and 8-OHdG are intracellular molecules that can be detected in extracellular body fluids, such as urine [39,50]. Above, we described changes in the levels of these molecules in vitreous fluids. To demonstrate the in situ regulation and production, we aimed to extend our findings with the use of immunohistochemical analysis. Immunofluorescence microscopy showed both nuclear and cytoplasmic 8-OHdG immunoreactivity in the untreated cells. HMGB1 treatment induced the upregulation of cytoplasmic and nuclear immunoreactivities (Figure 9B). Similarly, HMGB1 treatment induced the upregulation of HO-1 immunoreactivity in the cytoplasm of HRMECs (Figure 9C).

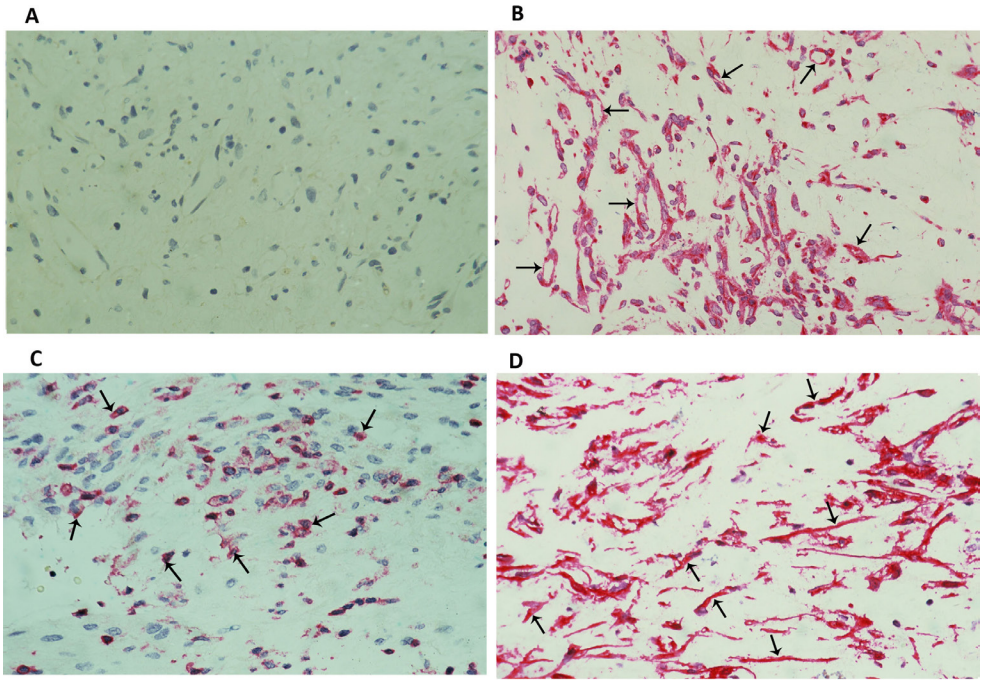

Figure 3. PDR epiretinal membrane immunostaining. Negative control slide showing no labeling **A**: immunohistochemical staining of CD31 showing blood vessels positive for this endothelial cell marker (arrows; **B**; original magnification 25X); immunohistochemical staining of CD45 showing stromal cells positive for CD45 (arrows; **C**); immunohistochemical staining of α-smooth muscle actin showing immunoreactivity in myofibroblasts (arrows; **D**; original magnification 40X).

DISCUSSION

Recently, HMGB1 has been recognized as an angiogenic cytokine [25-29]. In the present study, HMGB1 levels were significantly elevated in the vitreous fluid of patients with PDR. Furthermore, the levels were higher in patients with active PDR in comparison with patients with inactive PDR. In a previous study, we demonstrated that HMGB1 and RAGE were expressed by vascular endothelial and stromal cells in PDR epiretinal membranes and that significant correlations existed between the level of vascularization in PDR epiretinal membranes and the expressions of HMGB1 and RAGE [31]. In addition, we showed previously that stimulation with HMGB1 caused the upregulation of vascular endothelial growth factor (VEGF), a key angiogenic factor in PDR [53], in human retinal Müller cells [54]. Furthermore, HMGB1 induced HRMEC migration [54], a key early step in angiogenesis. Taken together, these findings suggest that the upregulation of HMGB1 in the ocular microenvironment of patients with PDR might contribute to the initiation and progression of angiogenesis associated with PDR.

It is well known that diabetic retinopathy is a chronic, low-grade subclinical inflammatory disorder. The adhesion of circulating leukocytes to the vascular endothelium is a key element of the proinflammatory phenotype assumed by the retinal microvasculature in diabetic retinopathy [3,4]. The retinal microvascular endothelial cells provide an important site of regulation and amplification of these inflammatory responses. Retinal endothelial cell activation leads to the enhanced adhesion of leukocytes to the retinal microvascular endothelium, retinal endothelial cell injuries, and the breakdown of the blood-retinal barrier [3,4]. Endothelial activation can be assessed by measuring the soluble (s) adhesion molecules ICAM-1, VCAM-1, and VAP-1 in the vitreous from patients with PDR. In general, vitreous fluid levels of sICAM-1 [8], sVCAM-1 [55], and sVAP-1 [56] are elevated in patients with PDR. In addition, the endothelial cell angiogenic markers soluble vascular endothelial-cadherin and soluble endoglin are upregulated in the vitreous fluid of patients with PDR [57]. Previous reports showed that HMGB1 mediates inflammatory responses by increasing the cell surface

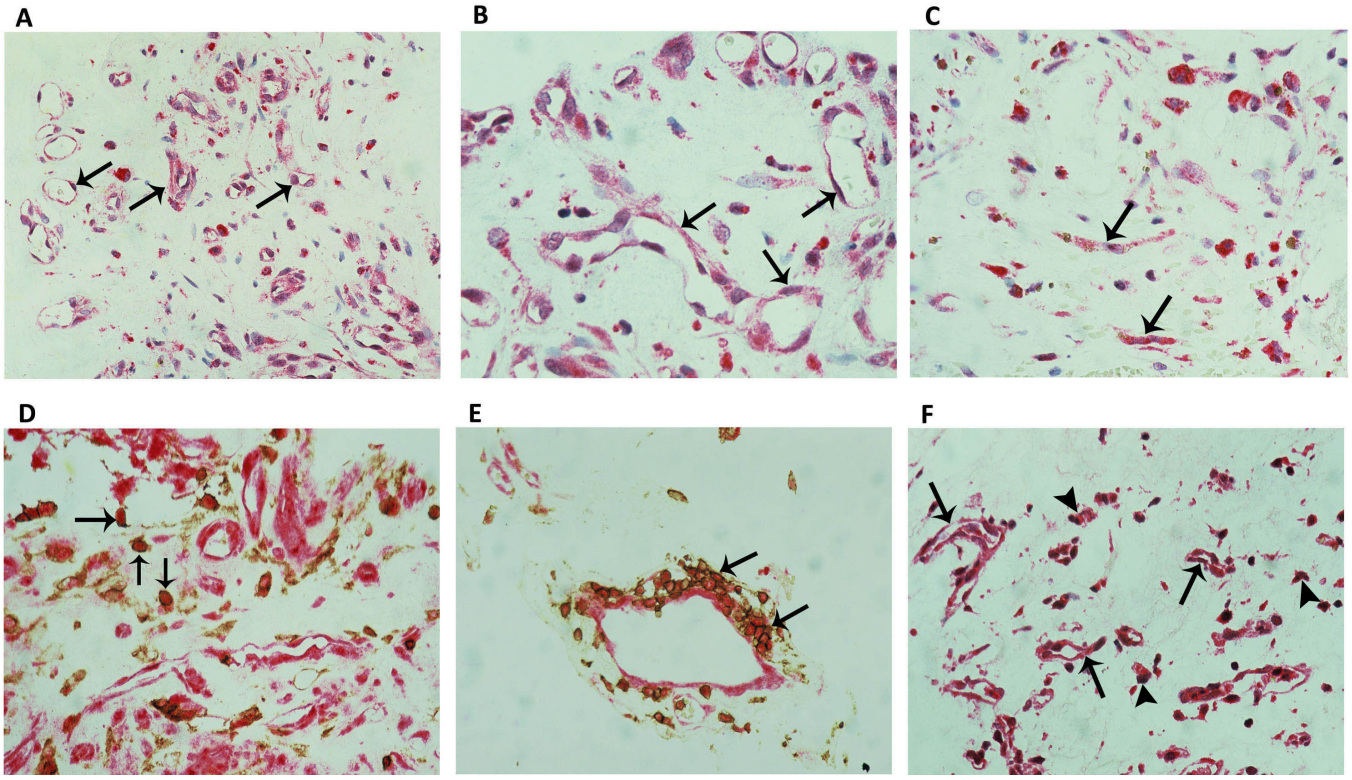

Figure 4. PDR epiretinal membrane immunostaining. Immunohistochemical staining of VAP-1 showing immunoreactivity in vascular endothelial cells (arrows) and stromal cells; low power (**A**: original magnification 25X) and high power (**B:** and **C:** original magnification 40X); stromal spindle-shaped cells expressed VAP-1 (arrows; **C**); double immunohistochemistry of CD45 (brown) and VAP-1 (red) showing stromal cells co-expressing CD45 and VAP-1 (arrows; **D** and **E**; original magnification X40); immunohistochemical staining of 8-OHdG showing nuclear and cytoplasmic immunoreactivities in vascular endothelial cells (arrows) and stromal cells (arrowheads; **F**: original magnification 25X).

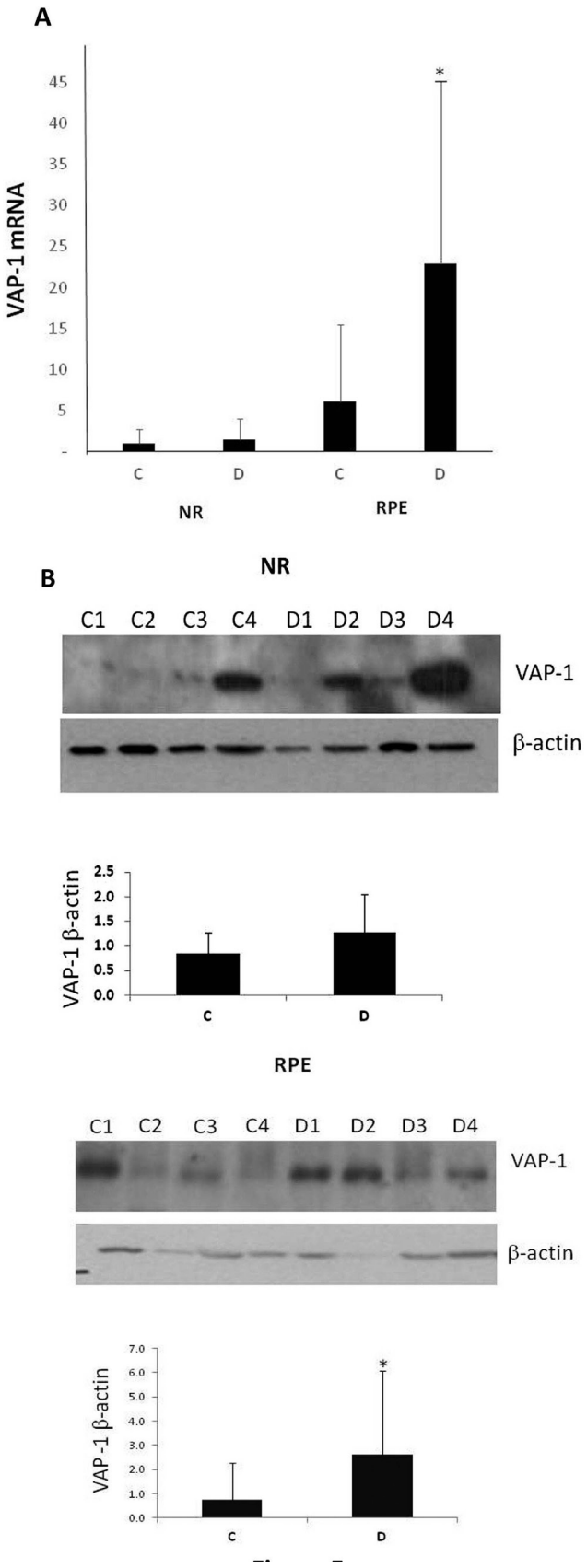

Figure 5. Expression of vascular adhesion protein-1 (VAP-1) in human retinas. **A**: mRNA was analyzed by real-time quantitative RT–PCR in the RPE and neuro-retina (NR). The VAP-1 mRNA expression was calculated after normalizing for β-actin mRNA levels. Bars represent the mean ± SD of the R.Q. values obtained for the mRNA levels in diabetic (**D**; n = 16) and non-diabetic control donors (**C**; n = 16). *p<0.05 (Mann–Whitney *U* test). **B**: The VAP-1 protein expression was determined by western blot analysis on lysates of the RPE and NR from representative diabetic (**D**; n = 4) and non-diabetic control (**C**; n = 4) donors. The ratios of band intensities of the VAP-1 protein versus actin were determined in all samples (n = 16/group). Data are expressed as the mean ± SD *p<0.05 (Mann–Whitney *U* test).

expressions of ICAM-1, VCAM-1, E-selectin, and P-selectin on the surface of endothelial cells, thereby promoting barrier disruption and the adhesion of leukocytes to HMGB1-activated endothelial cells and their subsequent migration [21-24]. This proinflammatory phenotype was mediated by the activation of NF-κB and was RAGE-dependent [23,24].

In the present study, we investigated the interactions of HMGB1 with HRMECs. Exogenous HMGB1 activates HRMECs to upregulate the adhesion molecule ICAM-1. These results are in agreement with our previous reports in which we demonstrated a significant correlation between the vitreous levels of HMGB1 and the levels of sICAM-1 in patients with PDR [8], and the intravitreal administration of HMGB1 induced significant upregulation of the expression of retinal ICAM-1 [32]. The expressions of VCAM-1 and VAP-1 were not affected by HMGB1 treatment. The elevated expression of ICAM-1 correlated with the enhanced binding of human leukocytes to HMGB1-activated HRMECs. ICAM-1 mediates the adhesion of leukocytes to the endothelium and subsequent transmigration to the sites of inflammation [58]. In addition, we demonstrated that the HMGB1 stimulation of HRMECs induced the membranous translocation of VAP-1. These results are consistent with previous reports that demonstrated the VAP-1 expression in the cytoplasm of endothelial cells in a non-inflamed state and that VAP-1 is rapidly translocated to a functional position on the endothelial cell surface in inflamed tissues [59,60]. The VAP-1 expression in the membrane of endothelial cells mediates the adhesion of leukocytes to the endothelium [61].

Oxidative stress occurs when the production of ROS exceeds the capacity of the cells to detoxify these injurious oxidants using endogenous antioxidant defense systems.

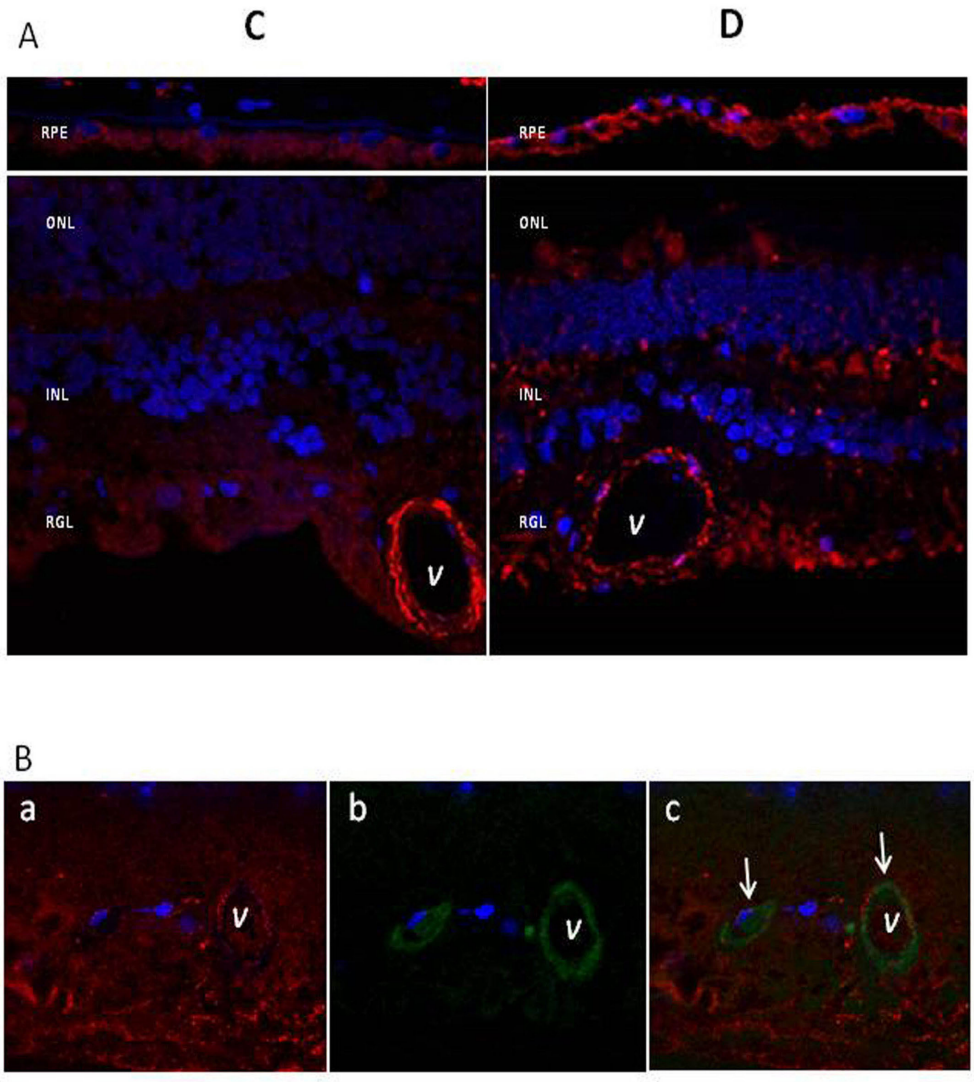

Figure 6. Microscopic analysis of VAP-1 in human retinas. **A**: Immunofluorescent staining of VAP-1 in representative samples from non-diabetic control (**C**) and diabetic (**D**) donors. After fixation, retinas were stained with a specific goat anti-VAP-1 antibody (red). Nuclei were labeled with DAPI (blue). RPE = retinal pigment epithelium; ONL = outer nuclear layer; INL = inner nuclear layer; RGL = ganglion cell layer. **B**: VAP-1 colocalized with collagen IV in human diabetic retinas. a: VAP-1 immunofluorescence (red). b: collagen IV immunofluorescence (green). c: VAP-1 (red), collagen IV (green), and nuclei (DAPI, blue). Orange fluorescence (white arrows) shows the colocalization of both forms of fluorescence in retinal vessels (V).

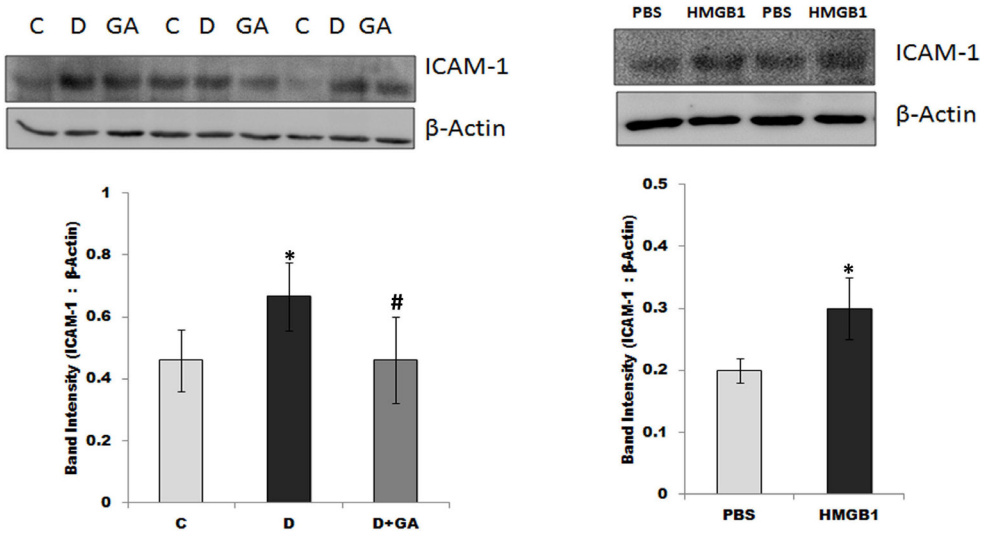

Figure 7. Western blot analysis of rat retinas. Diabetes caused a significant increase in the expression of ICAM-1 in the diabetic rats (**D**) compared to the non-diabetic controls (**C**; *p<0.05; Mann–Whitney *U* test). The diabetes-induced upregulation of ICAM-1 is attenuated in glycyrrhizic acid (GA)-fed diabetic rats (p<0.05; Mann–Whitney *U* test). The intravitreal administration of HMGB1 induced an upregulation of the expression of ICAM-1 compared to the intravitreal administration of PBS (*p<0.05; Mann–Whitney *U* test). A representative set of samples is shown. Results are expressed as the mean ± SD of 7–8 rats in each group.

Hyperglycemia-induced oxidative stress is linked to the pathophysiology of diabetic retinopathy [1,2,12]. Increased leukocyte-endothelial interactions, one of the hallmarks of diabetic retinopathy [1,2], is linked to the enhanced production of ROS [62]. ROS can promote a proinflammatory phenotype within the microvasculature through a variety of mechanisms, such as eliciting NF-κB activation, the increased production of inflammatory mediators (lipid mediators and cytokines), the increased expression of adhesion molecules on both the endothelium and circulating leukocytes, and increased leukocyte-endothelial adhesion [62]. In addition, increasing evidence suggests that ROS play an important role in angiogenesis via the hypoxia-inducible factor-1α/VEGF pathway [13,16]. Furthermore, oxidative stress is required for fibroblast activation and differentiation into a profibrotic α-SMA-expressing myofibroblast phenotype and this contributes to the pathogenesis of fibrosis in various organs [63-65].

In this study, we demonstrated increased levels of 8-OHdG in the vitreous fluid of PDR patients. In addition, we showed a significant positive correlation between vitreous fluid levels of HMGB1 and the levels of 8-OHdG. To corroborate these findings at the cellular level, stimulation with HMGB1 caused the upregulation of 8-OHdG in HRMECs. These findings suggest that increased HMGB1 is associated with oxidative stress in the ocular microenvironment of patients with PDR and the presence of a mechanistic link between HMGB1 and oxidative stress in the pathogenesis of PDR. In a previous study, we demonstrated a mutual enhancement between HMGB1 and nicotinamide adenine dinucleotide phosphate oxidase-derived ROS in diabetic retinas [12].

In the present study, vitreous levels of 8-OHdG were higher in PDR eyes with active neovascularization compared with eyes with inactive disease. These findings suggest that oxidative stress might promote an angiogenic response in the ocular microenvironment of patients with PDR. Our findings also suggest that elevated sVAP-1 levels in the vitreous fluid of patients with PDR may participate in the induction of oxidative stress in the ocular microenvironment of patients with PDR. Indeed, we observed a significant correlation between the levels of sVAP-1 and the levels of HMGB1 and the oxidative stress marker 8-OHdG in vitreous fluid.

In the present study, we report that the VAP-1 protein was specifically localized in vascular endothelial cells and stromal cells in epiretinal membranes from patients with PDR. In addition, sVAP-1 levels were higher in eyes with active neovascularization than in eyes with quiescent disease. It is likely that local VAP-1 production generates a local gradient of sVAP-1/hydrogen peroxide, which stimulates leukocyte migration and recruitment. Our findings are also consistent with previous reports that demonstrate how the catalytic oxidase activity of VAP-1 promotes angiogenic responses [44,66-68]. In addition, the catalytic oxidase activity of VAP-1 is strongly implicated in fibrotic diseases [43]. In the current study, the VAP-1 expression was unchanged in the neuroretinas of subjects with diabetes mellitus, in the retinas of diabetic rats, and in the retinas of normal rats after intravitreal HMGB1 administration. On the other hand, VAP-1 was upregulated in the RPE of human subjects with diabetes mellitus. Our findings are in agreement with previous studies that demonstrated an unchanged expression of VAP-1 in the

retinas of animals. In comparison, the ICAM-1 expression was upregulated in diabetic retinas [45].

In the current study, we detected the simultaneous expressions of HMGB1, 8-OHdG, and sVAP-1 in the vitreous fluid of patients with PDR. There were significant positive correlations between the levels of HMGB1 and the levels of 8-OHdG and sVAP-1 and between the levels of 8-OHdG and the levels of sVAP-1. These findings are in accordance with previous reports that demonstrated the active involvement of HMGB1 [12,30] and VAP-1 [40-42] in the generation of ROS. In a previous study, we demonstrated HMGB1 protein localization in vascular endothelial cells and stromal cells in epiretinal fibrovascular membranes from patients with PDR [31]. Similarly, in the present study, 8-OHdG and VAP-1 were localized in vascular endothelial and stromal cells in PDR epiretinal membranes. The colocalization of these biomarkers in the ocular microenvironment of patients with PDR suggests cross talk between these factors in the pathogenesis of PDR and that the co-expression of these factors is mechanistically interrelated.

In the current study, we demonstrated that stimulation with HMGB1 caused the upregulation of HO-1 in HRMECs. HO-1 levels were significantly higher in eyes with active neovascularization compared with eyes with involuted PDR, suggesting that HO-1 might contribute to PDR angiogenesis and progression. Indeed, several studies identified HO-1 and its gaseous product, carbon monoxide, as possessing potent pro-angiogenic properties, in addition to well-described

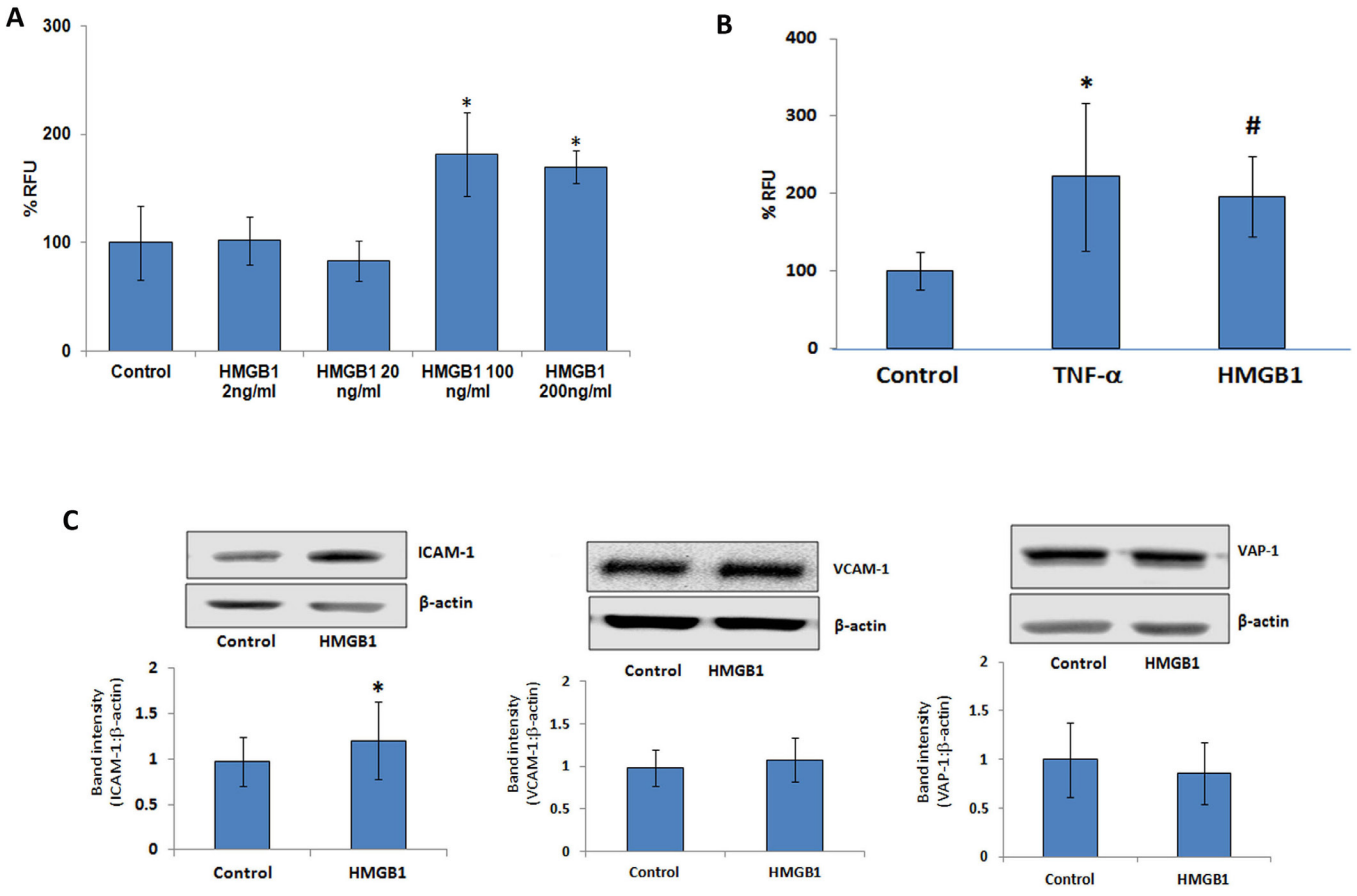

Figure 8. HMGB1 induces leukocyte adhesion to HRMECs and the expressions of cell adhesion molecules. **A**: The dose-dependent effects of rh HMGB1 on leukocyte adhesion. HRMEC monolayers in 96-well plates were treated with different doses of HMGB1 for 24 h and then LeukoTracker-labeled human leukocytes were allowed to attach to HRMEC for 30 min. Adherent cells were lysed and quantified as described in the method section. Each group has at least three wells. **B**: TNF-α (1 ng/ml; *p<0.05; Mann–Whitney *U* test) and HMGB1 (100 ng/ml; #p<0.05; Mann–Whitney *U* test) induced human leukocyte adhesion to HRMEC monolayers. The bar graph represents three independent experiments (control 10 wells, TNF-α 6 wells, HMGB1 10 wells). RFU = relative fluorescent unit. **C**: Effects of HMGB1 on the expressions of ICAM-1, VCAM-1, and VAP-1 on HRMECs. The protein expressions of ICAM-1, VCAM-1, and VAP-1 in treated and untreated (control) cell lysates were determined by western blot analysis. Western blots are representative of at least three independent experiments, each performed in triplicate, and bar graphs are representative of all three experiments. (*p<0.05; Mann-Whitney U test).

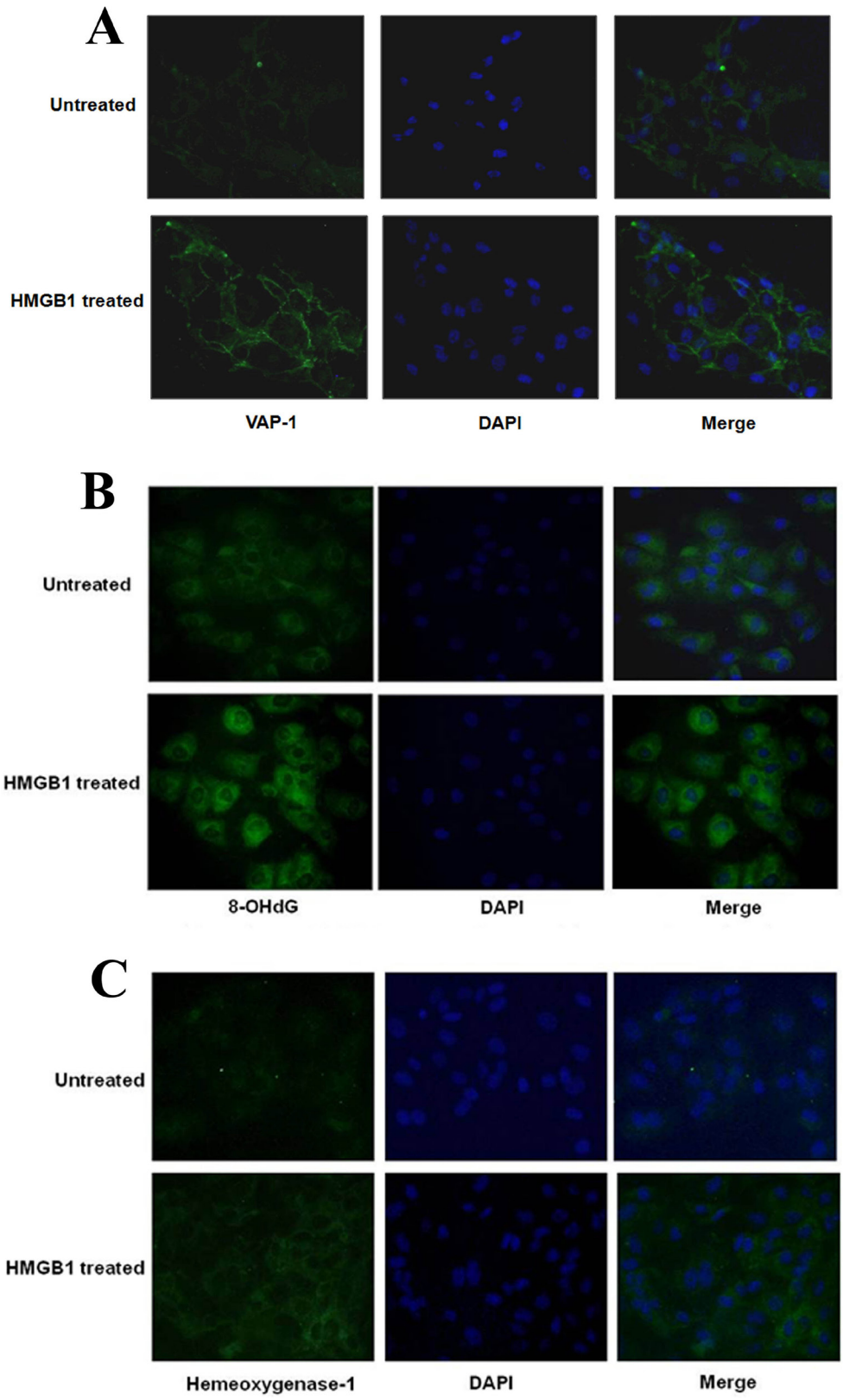

Figure 9. Effects of HMGB1 on the expressions of VAP-1, 8-OHdG, and HO-1 in human retinal microvascular endothelial cells. Immunofluorescence microscopy showed that HMGB1 treatment induced membranous VAP-1 translocation (**A**), the upregulation of cytoplasmic and nuclear immunoreactivities for 8-OHdG (**B**), and cytoplasmic immunoreactivity for HO-1 (**C**; green). Nuclei were counterstained with DAPI (blue).

anti-inflammatory, antioxidant, and anti-apoptotic effects. HO-1 enhances endothelial cell and endothelial progenitor cell survival, proliferation, migration, and tube formation (46, 47, 70). Moreover, angiogenic factors, such as VEGF, mediate their pro-angiogenic effects through the induction of HO-1, which also induces the synthesis of VEGF, resulting in a positive feedback loop [69,70]. Thus, in PDR associated with VEGF-driven angiogenesis, HO-1 may act to enhance angiogenesis.

In conclusion, our findings suggest a potential link among HMGB1 and VAP-1, oxidative stress, and HO-1 in the pathogenesis of inflammation and angiogenesis associated with PDR. Modulating the activity of HMGB1 may provide a novel approach for treating diabetic retinopathy.

ACKNOWLEDGMENTS

The authors thank Mr. Wilfried Versin and Ms. Nathalie Volders technical assistance; and Ms. Connie B. Unisa-Marfil for secretarial work. This work was supported by King Saud University through Vice Deanship of Research Chair (Dr. Nasser Al-Rashid Research Chair in Ophthalmology, Abu El-Asrar AM). GO is supported by the Research Foundation of Flanders (FWO-Vlaanderen) and by the concerted research actions at KU Leuven (GOA 2013/015).

REFERENCES

1. Kowluru RA, Kowluru A, Mishra M, Kumar B. Oxidative stress and epigenetic modifications in the pathogenesis of diabetic retinopathy. Prog Retin Eye Res 2015; 48:40-61. [PMID: 25975734].

2. Behl T, Kaur I, Kotwani A. Implication of oxidative stress in progression of diabetic retinopathy. Surv Ophthalmol 2016; 61:187-96. [PMID: 26074354].

3. Miyamoto K, Khosrof S, Bursell SE, Rohan R, Murata T, Clermont AC, Aiello LP, Ogura Y, Adamis AP. Prevention of leukostasis and vascular leakage in streptozotocin-induced diabetic retinopathy via intercellular adhesion molecule-1 inhibition. Proc Natl Acad Sci USA 1999; 96:10836-41. [PMID: 10485912].

4. Joussen AM, Poulaki V, Le ML, Koizumi K, Esser C, Janicki H, Schraermeyer U, Kociok N, Fauser S, Kirchhof B, Kern TS, Adamis AP. A central role for inflammation in the pathogenesis of diabetic retinopathy. FASEB J 2004; 18:1450-2. [PMID: 15231732].

5. Abu El-Asrar AM, De Hertogh G, van den Eynde K, Alam K, Van Raemdonck K, Opdenakker G, Struyf S. Myofibroblasts in proliferative diabetic retinopathy can originate from infiltrating fibrocytes and through endothelial-to-mesenchymal transition (EndoMT). Exp Eye Res 2015; 132:179-89. [PMID: 25637870].

6. Abu El-Asrar AM, Nawaz MI, De Hertogh G, Alam K, Siddiquei MM, Van den Eynde K, Opdenakker G. S100A4 is upregulated in proliferative diabetic retinopathy and correlates with markers of angiogenesis and fibrogenesis. Mol Vis 2014; 20:1209-24. [PMID: 25253987].

7. Abu El-Asrar AM, Nawaz MI, Kangave D, Siddiquei MM, Geboes K. Angiogenic and vasculogenic factors in the vitreous from patients with proliferative diabetic retinopathy. J Diabetes Res 2013; 2013:539658:[PMID: 23671874].

8. El-Asrar AM, Nawaz MI, Kangave D, Geboes K, Ola MS, Ahmad S, Al-Shabrawey M. High-mobility group box-1and biomarkers of inflammation in the vitreous from patients with proliferative diabetic retinopathy. Mol Vis 2011; 17:1829-38. [PMID: 21850157].

9. Nawaz MI, Van Raemdonck K, Mohammad G, Kangave D, Van Damme J, Abu El-Asrar AM, Struyf S. Autocrine CCL2, CXCL4, CXCL9 and CXCL10 signal in retinal endothelial cells and are enhanced in diabetic retinopathy. Exp Eye Res 2013; 109:67-76. [PMID: 23352833].

10. Abu El-Asrar AM, Mohammad G, Nawaz MI, Siddique MM, Van den Eynde K, Mousa A, De Hertogh G, Opdenakker G. Relationship between vitreous levels of matrix metalloproteinases and vascular endothelial growth factor in proliferative diabetic retinopathy. PLoS One 2013; 8:e85857-[PMID: 24392031].

11. Abu El-Asrar AM, Alam K, Nawaz MI, Mohammad G, Van den Eynde K, Siddiquei MM, Mousa A, De Hertogh G, Geboes K, Opdenakker G. Upregulated expression of heparanase in the vitreous of patients with proliferative diabetic retinopathy originates from activated endothelial cells and leukocytes. Invest Ophthalmol Vis Sci 2015; 56:8239-47. [PMID: 26720478].

12. Mohammad G, Alam K, Nawaz MI, Siddiquei MM, Mousa A, Abu El-Asrar AM. Mutual enhancement between high-mobility group box-1 and NADPH oxidase-derived reactive oxygen species mediates diabetes-induced upregulation of retinal apoptotic markers. J Physiol Biochem 2015; 71:359-72. [PMID: 26040511].

13. Kim YW, Byzova TV. Oxidative stress in angiogenesis and vascular disease. Blood 2014; 123:625-31. [PMID: 24300855].

14. Kim YW, West XZ, Byzova TV. Inflammation and oxidative stress in angiogenesis and vascular disease. J Mol Med (Berl) 2013; 91:323-8. [PMID: 23430240].

15. Ono M. Molecular links between tumor angiogenesis and inflammation: inflammatory stimuli of macrophages and cancer cells as targets for therapeutic strategy. Cancer Sci 2008; 99:1501-6. [PMID: 18754859].

16. Ushio-Fukai M, Nakamura Y. Reactive oxygen species and angiogenesis: NADPH oxidase as target for cancer therapy. Cancer Lett 2008; 266:37-52. [PMID: 18406051].

17. Orlova VV, Choi EY, Xie C, Chavakis E, Bierhaus A, Ihanus E, Ballantyne CM, Gahmberg CG, Bianchi ME, Nawroth PP, Chavakis T. A novel pathway of HMGB1-mediated

inflammatory cell recruitment that requires Mac-1-integrin. EMBO J 2007; 26:1129-39. [PMID: 17268551].

18. van Beijnum JR, Buurman WA, Griffioen AW. Convergence and amplification of toll-like receptor (TLR) and receptor for advanced glycation end products (RAGE) signaling pathways via high mobility group B1 (HMGB1). Angiogenesis 2008; 11:91-9. [PMID: 18264787].

19. Venereau E, Schiraldi M, Uguccioni M, Bianchi ME. HMGB1 and leukocyte migration during trauma and sterile inflammation. Mol Immunol 2013; 55:76-82. [PMID: 23207101].

20. Schiraldi M, Raucci A, Muñoz LM, Livoti E, Celona B, Venereau E, Apuzzo T, De Marchis F, Pedotti M, Bachi A, Thelen M, Varani L, Mellado M, Proudfoot A, Bianchi ME, Uguccioni M. HMGB1 promotes recruitment of inflammatory cells to damaged tissues by forming a complex with CXCL12 and signaling via CXCR4. J Exp Med 2012; 209:551-63. [PMID: 22370717].

21. Liu Z, Wang Z, Han G, Huang L, Jiang J, Li S. Ketamine attenuates high mobility group box-1-induced inflammatory responses in endothelial cells. J Surg Res 2016; 200:593-603. [PMID: 26453003].

22. Fiuza C, Bustin M, Talwar S, Tropea M, Gerstenberger E, Shelhamer JH, Suffredini AF. Inflammation-promoting activity of HMGB1 on human microvascular endothelial cells. Blood 2003; 101:2652-60. [PMID: 12456506].

23. Treutiger CJ, Mullins GE, Johansson AS, Rouhiainen A, Rauvala HM, Erlandsson-Harris H, Andersson U, Yang H, Tracey KJ, Andersson J, Palmblad JE. High mobility group 1 B-box mediates activation of human endothelium. J Intern Med 2003; 254:375-85. [PMID: 12974876].

24. Luo Y, Li SJ, Yang J, Qiu YZ, Chen FP. HMGB1 induces an inflammatory response in endothelial cells via the RAGE-dependent endoplasmic reticulum stress pathway. Biochem Biophys Res Commun 2013; 438:732-8. [PMID: 23911608].

25. van Beijnum JR, Nowak-Sliwinska P, van den Boezem E, Hautvast P, Buurman WA, Griffioen AW. Tumor angiogenesis is enforced by autocrine regulation of high-mobility group box 1. Oncogene 2013; 32:363-74. [PMID: 22391561].

26. Mitola S, Belleri M, Urbinati C, Coltrini D, Sparatore B, Pedrazzi M, Melloni E, Presta M. Cutting edge: extracellular high mobility group box-1 protein is a proangiogenic cytokine. J Immunol 2006; 176:12-5. [PMID: 16365390].

27. Schlueter C, Weber H, Meyer B, Rogalla P, Röser K, Hauke S, Bullerdiek J. Angiogenetic signaling through hypoxia. HMGB1: an angiogenic switch molecule. Am J Pathol 2005; 166:1259-63. [PMID: 15793304].

28. Chavakis E, Hain A, Vinci M, Carmona G, Bianchi ME, Vajkoczy P, Zeiher AM, Chavakis T, Dimmeler S. High-mobility group box 1 activates integrin-dependent homing of endothelial progenitor cells. Circ Res 2007; 100:204-12. [PMID: 17218606].

29. van Beijnum JR, Dings RP, van der Linden E, Zwaans BM, Ramaekers FC, Mayo KH, Griffioen AW. Gene expression of tumor angiogenesis dissected: specific targeting of colon cancer angiogenic vasculature. Blood 2006; 108:2339-48. [PMID: 16794251].

30. Tang D, Kang R, Zeh HJ 3rd, Lotze MT. High-mobility group box 1, oxidative stress, and disease. Antioxid Redox Signal 2011; 14:1315-35. [PMID: 20969478].

31. El-Asrar AM, Missotten L, Geboes K. Expression of high-mobility groups box-1/receptor for advanced glycation end products/osteopontin/early growth response-1 pathway in proliferative vitreoretinal epiretinal membranes. Mol Vis 2011; 17:508-18. [PMID: 21365018].

32. Mohammad G, Siddiquei MM, Othman A, Al-Shabrawey M, Abu El-Asrar AM. High-mobility group box-1 protein activates inflammatory signaling pathway components and disrupts retinal vascular-barrier in the diabetic retina. Exp Eye Res 2013; 107:101-9. [PMID: 23261684].

33. Abu El-Asrar AM, Siddiquei MM, Nawaz MI, Geboes K, Mohammad G. The proinflammatory cytokine high-mobility group box-1 mediates retinal neuropathy induced by diabetes. Mediators Inflamm 2014; 2014:746415-[PMID: 24733965].

34. Abu El-Asrar AM, Mohammad G, Nawaz MI, Siddiquei MM. High-Mobility Group Box-1 Modulates the Expression of Inflammatory and Angiogenic Signaling Pathways in Diabetic Retina. Curr Eye Res 2015; 40:1141-52. [PMID: 25495026].

35. Abu El-Asrar AM, Nawaz MI, Siddiquei MM, Al-Kharashi AS, Kangave D, Mohammad G. High-mobility group box-1 induces decreased brain-derived neurotrophic factor-mediated neuroprotection in the diabetic retina. Mediators Inflamm 2013; 2013:863036-[PMID: 23766563].

36. Di Minno A, Turnu L, Porro B, Squellerio I, Cavalca V, Tremoli E, Di Minno MN. 8-Hydroxy-2-Deoxyguanosine Levels and Cardiovascular Disease: A Systematic Review and Meta-Analysis of the Literature. Antioxid Redox Signal 2016; 24:548-55. [PMID: 26650622].

37. Kroese LJ, Scheffer PG. 8-hydroxy-2′-deoxyguanosine and cardiovascular disease: a systematic review. Curr Atheroscler Rep 2014; 16:452-60. [PMID: 25252787].

38. Wu LL, Chiou CC, Chang PY, Wu JT. Urinary 8-OHdG: a marker of oxidative stress to DNA and a risk factor for cancer, atherosclerosis and diabetics. Clin Chim Acta 2004; 339:1-9. [PMID: 14687888].

39. Moresco RN, Sangoi MB, De Carvalho JA, Tatsch E, Bochi GV. Diabetic nephropathy: traditional to proteomic markers. Clin Chim Acta 2013; 421:17-30. [PMID: 23485645].

40. Pannecoeck R, Serruys D, Benmeridja L, Delanghe JR, van Geel N, Speeckaert R, Speeckaert MM. Vascular adhesion protein-1: Role in human pathology and application as a biomarker. Crit Rev Clin Lab Sci 2015; 52:284-300. [PMID: 26287391].

41. Jalkanen S, Karikoski M, Mercier N, Koskinen K, Henttinen T, Elima K, Salmivirta K, Salmi M. The oxidase activity of vascular adhesion protein-1 (VAP-1) induces endothelial E- and P-selectins and leukocyte binding. Blood 2007; 110:1864-70. [PMID: 17548577].

42. Yu PH, Wright S, Fan EH, Lun ZR, Gubisne-Harberle D. Physiological and pathological implications of semicarbazide-sensitive amine oxidase. Biochim Biophys Acta 2003; 1647:193-9. [PMID: 12686132].

43. Weston CJ, Shepherd EL, Claridge LC, Rantakari P, Curbishley SM, Tomlinson JW, Hubscher SG, Reynolds GM, Aalto K, Anstee QM, Jalkanen S, Salmi M, Smith DJ, Day CP, Adams DH. Vascular adhesion protein-1 promotes liver inflammation and drives hepatic fibrosis. J Clin Invest 2015; 125:501-20. [PMID: 25562318].

44. Yoshikawa N, Noda K, Ozawa Y, Tsubota K, Mashima Y, Ishida S. Blockade of vascular adhesion protein-1 attenuates choroidal neovascularization. Mol Vis 2012; 18:593-600. [PMID: 22419852].

45. Noda K, Nakao S, Zandi S, Engelstädter V, Mashima Y, Hafezi-Moghadam A. Vascular adhesion protein-1 regulates leukocyte transmigration rate in the retina during diabetes. Exp Eye Res 2009; 89:774-81. [PMID: 19635478].

46. Loboda A, Jozkowicz A, Dulak J. HO-1/CO system in tumor growth, angiogenesis and metabolism - Targeting HO-1 as an anti-tumor therapy. Vascul Pharmacol 2015; 74:11-22. [PMID: 26392237].

47. Dulak J, Deshane J, Jozkowicz A, Agarwal A. Heme oxygenase-1 and carbon monoxide in vascular pathobiology: focus on angiogenesis. Circulation 2008; 117:231-41. [PMID: 18195184].

48. Fan J, Xu G, Jiang T, Qin Y. Pharmacologic induction of heme oxygenase-1 plays a protective role in diabetic retinopathy in rats. Invest Ophthalmol Vis Sci 2012; 53:6541-56. [PMID: 22661484].

49. Dietrich N, Kolibabka M, Busch S, Bugert P, Kaiser U, Lin J, Fleming T, Morcos M, Klein T, Schlotterer A, Hammes HP. The DPP4 Inhibitor Linagliptin Protects from Experimental Diabetic Retinopathy. PLoS One 2016; 11:e0167853-[PMID: 27942008].

50. Li Z, Xu Y, Liu X, Nie Y, Zhao Z. Urinary heme oxygenase-1 as a potential biomarker for early diabetic nephropathy. Nephrology (Carlton) 2017; 22:58-64. [PMID: 26733347].

51. Aiello LP, Avery RL, Arrigg PG, Keyt BA, Jampel HD, Shah ST, Pasquale LR, Thieme H, Iwamoto MA, Park JE, Nguyen HV, Aiello LM, Ferrara N, King GL. Vascular endothelial growth factor in ocular fluid of patients with diabetic retinopathy and other retinal disorders. N Engl J Med 1994; 331:1480-7. [PMID: 7526212].

52. Mollica L, De Marchis F, Spitaleri A, Dallacosta C, Pennacchini D, Zamai M, Agresti A, Trisciuglio L, Musco G, Bianchi ME. Glycyrrhizin binds to high-mobility group box 1 protein and inhibits its cytokine activities. Chem Biol 2007; 14:431-41. [PMID: 17462578].

53. Spranger J, Pfeiffer AF. New concepts in pathogenesis and treatment of diabetic retinopathy. Exp Clin Endocrinol Diabetes 2001; 109:Suppl 2S438-50. [PMID: 11460590].

54. Mohammad G, Jomar D, Siddiquei MM, Alam K, Abu El-Asrar AM. High-Mobility Group Box-1 Protein Mediates the Regulation of Signal Transducer and Activator of Transcription-3 in the Diabetic Retina and in Human Retinal Müller Cells. Ophthalmic Res 2017; 57:150-60. [PMID: 27560926].

55. Abu El-Asrar AM, Nawaz MI, Mohammad G, Siddiquei MM, Alam K, Mousa A, Opdenakker G. Expression of bioactive lysophospholipids and processing enzymes in the vitreous from patients with proliferative diabetic retinopathy. Lipids Health Dis 2014; 13:187-[PMID: 25496321].

56. Murata M, Noda K, Fukuhara J, Kanda A, Kase S, Saito W, Ozawa Y, Mochizuki S, Kimura S, Mashima Y, Okada Y, Ishida S. Soluble vascular adhesion protein-1 accumulates in proliferative diabetic retinopathy. Invest Ophthalmol Vis Sci 2012; 53:4055-62. [PMID: 22618595].

57. Abu El-Asrar AM, Nawaz MI, Kangave D, Abouammoh M, Mohammad G. High-mobility group box-1 and endothelial cell angiogenic markers in the vitreous from patients with proliferative diabetic retinopathy. Mediators Inflamm 2012; 2012:697489-[PMID: 23118492].

58. Haraldsen G, Kvale D, Lien B, Farstad IN, Brandtzaeg P. Cytokine-regulated expression of E-selectin, intercellular adhesion molecule-1 (ICAM-1), and vascular cell adhesion molecule-1 (VCAM-1) in human microvascular endothelial cells. J Immunol 1996; 156:2558-65. [PMID: 8786319].

59. Jaakkola K, Nikula T, Holopainen R, Vähäsilta T, Matikaine MT, Laukkanen ML, Huupponen R, Halkola L, Nieminen L, Hiltunen J, Parviainen S, Clark MR, Knuuti J, Savunen T, Kaapa P, Voipio-Pulkki LM, Jalkanen S. In vivo detection of vascular adhesion protein-1 in experimental inflammation. Am J Pathol 2000; 157:463-71. [PMID: 10934150].

60. Vainio PJ, Kortekangas-Savolainen O, Mikkola JH, Jaakkola K, Kalimo K, Jalkanen S, Veromaa T. Safety of blocking vascular adhesion protein-1 in patients with contact dermatitis. Basic Clin Pharmacol Toxicol 2005; 96:429-35. [PMID: 15910406].

61. Sole M, Unzeta M. Vascular cell lines expressing SSAO/VAP-1: a new experimental tool to study its involvement in vascular diseases. Biol Cell 2011; 103:543-57. [PMID: 21819380].

62. Cooper D, Stokes KY, Tailor A, Granger DN. Oxidative stress promotes blood cell-endothelial cell interactions in the microcirculation. Cardiovasc Toxicol 2002; 2:165-80. [PMID: 12665663].

63. Barnes JL, Gorin Y. Myofibroblast differentiation during fibrosis: role of NAD(P)H oxidases. Kidney Int 2011; 79:944-56. [PMID: 21307839].

64. Cui Y, Robertson J, Maharaj S, Waldhauser L, Niu J, Wang J, Farkas L, Kolb M, Gauldie J. Oxidative stress contributes to the induction and persistence of TGF-β1 induced pulmonary fibrosis. Int J Biochem Cell Biol 2011; 43:1122-33. [PMID: 21514399].

65. Zhao W, Zhao T, Chen Y, Ahokas RA, Sun Y. Oxidative stress mediates cardiac fibrosis by enhancing transforming growth factor-beta1 in hypertensive rats. Mol Cell Biochem 2008; 317:43-50. [PMID: 18581202].

66. Marttila-Ichihara F, Auvinen K, Elima K, Jalkanen S, Salmi M. Vascular adhesion protein-1 enhances tumor growth by supporting recruitment of Gr-1^{+}CD11b^{+} myeloid cells into tumors. Cancer Res 2009; 69:7875-83. [PMID: 19789345].

67. Li R, Li H, Luo HJ, Lin ZX, Jiang ZW, Luo WH. SSAO inhibitors suppress hepatocellular tumor growth in mice. Cell Immunol 2013; 283:61-9. [PMID: 23850964].

68. Marttila-Ichihara F, Castermans K, Auvinen K, Oude Egbrink MG, Jalkanen S, Griffioen AW, Salmi M. Small-molecule inhibitors of vascular adhesion protein-1 reduce the accumulation of myeloid cells into tumors and attenuate tumor growth in mice. J Immunol 2010; 184:3164-73. [PMID: 20154208].

69. Bussolati B, Ahmed A, Pemberton H, Landis RC, Di Carlo F, Haskard DO, Mason JC. Bifunctional role for VEGF-induced heme oxygenase-1 in vivo: induction of angiogenesis and inhibition of leukocytic infiltration. Blood 2004; 103:761-6. [PMID: 14525760].

70. Bussolati B, Mason JC. Dual role of VEGF-induced heme-oxygenase-1 in angiogenesis. Antioxid Redox Signal 2006; 8:1153-63. [PMID: 16910763].

Articles are provided courtesy of Emory University and the Zhongshan Ophthalmic Center, Sun Yat-sen University, P.R. China. The print version of this article was created on 5 December 2017. This reflects all typographical corrections and errata to the article through that date. Details of any changes may be found in the online version of the article.